

Article

Increasing Wind Speeds Fuel the Wider Spreading of Pollution Caused by Fires over the IGP Region during the Indian Post-Monsoon Season

Vinay Kumar ¹, Rupesh Patil ², Rohini L. Bhawar ^{3,*}, P.R.C. Rahul ⁴ and Subbarao Yelisetti ¹¹ Department of Physics and Geosciences, Texas A & M University, Kingsville, TX 78363, USA² Maharashtra Education Society Abasaheb Garware College, Pune 411004, India³ Department of Atmospheric and Space Sciences, Savitribai Phule Pune University, Pune 411008, India⁴ Indian Institute of Tropical Meteorology, Pune 411008, India

* Correspondence: rbhawar@unipune.ac.in; Tel.: +91-20-25691712

Abstract: Every year, forest fires and harvest harnessing produce atmospheric pollution in October and November over the Indo-Gangetic Plain (IGP). The fire count data (MODIS) shows a decreasing/increasing trend of fire counts in all confidence ranges in October/November over Northern India. There is a widespread increase in fires with a confidence level above 60 to 80% over the whole Northern Indian region. The Aerosol Optical Index (AOD) also shows an increase with values > 0.7 over the northwestern and IGP regions. There have been some startling results over the lower IGP belt, where there has been increasing trend in AOD during October ~56% and during November, the increase was by a whopping ~116%. However, in November, a slight turning of the winds towards central India might be transporting the AOD towards the central Indian region. Hence, during November, it is inferred that due to the low wind speed over the lower IGP belt and increased fires, the AODs in the polluted air tend to hover for a long time. During recent years from 2010, the winds have become stronger, indicating more transport of AOD is occurring over the lower IGP belt as compared to previous years till 2009, especially in October.

Keywords: IGP; fire counts; AOD; pollution

Citation: Kumar, V.; Patil, R.; Bhawar, R.L.; Rahul, P.R.C.; Yelisetti, S. Increasing Wind Speeds Fuel the Wider Spreading of Pollution Caused by Fires over the IGP Region during the Indian Post-Monsoon Season. *Atmosphere* **2022**, *13*, 1525. <https://doi.org/10.3390/atmos13091525>

Academic Editor: Ashok Luhar

Received: 11 August 2022

Accepted: 15 September 2022

Published: 18 September 2022

Publisher's Note: MDPI stays neutral with regard to jurisdictional claims in published maps and institutional affiliations.



Copyright: © 2022 by the authors. Licensee MDPI, Basel, Switzerland. This article is an open access article distributed under the terms and conditions of the Creative Commons Attribution (CC BY) license (<https://creativecommons.org/licenses/by/4.0/>).

1. Introduction

The Indo-Gangetic Plain (IGP) region is a prominent part of northern India and also an aggressive domain for pollution increase over a tropical belt. The IGP region remains a region of interest due to its uniqueness in rainfall variability, aerosol variations, and basin of nine rivers, and also due to the menacing problem of enhanced pollution caused by crop residue burning. In recent times, the IGP region has also become the most polluted region in India [1] and is counted as one, among the top worldwide. The variations over the IGP region have had counterproductive negative effects on the snow-clad mountains that form the northern part of India [2]. The IGP region has a double blanket (two layers) of black carbon, causing significant implications in the heating rates and the melting of snow over the Tibetan plateau [3]. In fact, the IGP region covers almost 300,000 km square of fertile area, which makes it an important region that needs extensive research work to be carried out.

Biomass burning, which is reflected as fire counts, is a major source of carbonaceous aerosols that play a crucial role in the radiation budget, air quality, ecosystems, human health, and climate [4–6]. Further, it is affecting the atmospheric radiative phenomenon at various scales, from local emissions to long-range transport mechanisms [7,8]. Biomass burning is a major global source of fine carbonaceous aerosols [9]. Several factors, such as man-made fires, agricultural burning, deforestation, and biofuel combustion, contribute to biomass burning aerosols spewing into the atmosphere. These aerosols emitted through

biomass burning affect the Earth's climate system via both direct and indirect effects [10]. Moreover, these aerosols warm the atmosphere and cool the Earth's surface and often modify cloud microphysical properties by acting as ice nuclei [11–17]. Some studies indicate that biomass-burning aerosols have been known to cause severe environmental pollution over the regions they hover and more seriously damage the health of the otherwise normal healthy human population [17]. The severity of such contaminated air in overpopulated areas was revealed in a recent study over six IGP regions in terms of severe aerosol loading ($AOD_{500} > 1.0$), high values of Ångström exponent (>1.2), and high particulate matter ($PM_{2.5}$) concentrations ($>100\text{--}150 \mu\text{g m}^{-3}$) [8]. The smoke aerosols are known to be transported to distances as far as 600 km away from their sources of origin. They have also been found to exist as elevated aerosol layers of up to 3–5 km [18,19]. The key global source regions of biomass burning aerosols have been identified as sub-Saharan Africa, South America, Southeast Asia, Northern Australia, and the boreal forest in the northern hemisphere [20,21]. NASA A-train satellite sensors detected post-harvest agricultural fire activity (net ~60%), leading to a nearly 43% increase in aerosol loading over the populated IGP in northern India [22]. In India, maximum forest fire counts occur during the pre-monsoon season (March to May), while residual burning occurs in the dual-phase season, pre-monsoon season (April to May), and post-monsoon season (October to November). Biomass-burning smoke plumes damage the on-air quality more during winter as the plumes are trapped in the lower troposphere. The favorable low temperatures, result in dense fog conditions over the entire IGP region, and often, in many cases, these smoke plumes reach central India and the Bay of Bengal [23,24]. Crop residue burning over northwestern India is recognized to pose a serious health concern on a disastrous scale, affecting the health of millions of people in this densely populated region of the world. Major cities in the IGP region have registered a consistent ranking for the poorest air quality from the World Meteorological Organization (WMO), especially related to particulate matter concentrations.

This study pinpoints an increasing trend in the fire counts from the analysis of data studied for approximately two decades (2002–2019). We further investigate the cause of the spread of deteriorating unhealthy air over the IGP region. Though the earlier study pointed out that an increase in the fire counts is related to the greater availability of crop residue to burn and is proportional to the waste generated and the crop production amounts [22]. This study, for the first time, probes and proves that the wind patterns have played and will be playing an all-important role in the spread of toxic air throughout the IGP region.

2. Materials and Methods

2.1. Study Area

This study covered the northern Indian subcontinent region, which is quite large ($60\text{--}90^\circ \text{ E}$; $20\text{--}40^\circ \text{ N}$). However, AOD climatology, fire counts, and winds show a prominent impact on IGP, hence, in this study, the focus is exclusively over the IGP region.

2.2. Analysis of Satellite Datasets

In this present study, data has been considered from MODIS onboard the AQUA satellite orbiting in a near-polar orbit. The Moderate Resolution Imaging Spectroradiometer (MODIS) measures radiances at 36 wavelengths from 0.41 to 14 μm and provides near-global coverage every day. The MODIS AOD data [25,26] is taken from the monthly mean level 3 products (MYD08-6.1) with a 1×1 -degree resolution for the period 2002–2019 (<https://giovanni.gsfc.nasa.gov/giovanni/>) (accessed on 14 September 2022). For the time series analysis plot, we have area-averaged the aerosol optical depth data for the study region. The fire confidence data from MODIS was considered to understand the spatial distribution of fires. We have used the fire data above a 50-confidence level in different groups to understand the spatial fire variability in a particular group. Time series analysis of the fire confidence data in different groups is also done for different regions considered in this study. The vertical velocity and wind vector data at 850 hPa are considered from the

NCEP reanalysis for the period of 2002–2019, while rainfall and moisture datasets are from 2002 to 2021.

3. Results and Discussions

The post-monsoon season contributes heavily to biomass burning [27], and hence these time scales have been selected for a clear perspective. We present, in Figure 1, the AOD climatology from 2002–2019 (18 years) obtained from the MODIS-AQUA satellite during the post-monsoon months of October (Figure 1a) and November (Figure 1b). During this time, it is seen that the northern belt over India is starkly infused with high values of AODs as high as 1, beginning with values of 0.4 during the months of October and November over IGP. Some of the pockets of the IGP, especially the Northern Punjab region, show very high values of AOD during October, as this is the time for harvesting and burning of residuals. The uncertainties in this research might be increased due to the comparison of datasets from diverse resolutions. The fire count does not provide a clue about the size of the fire. Biomass burning emissions are reflected as the fire counts are predominantly dominated by the crop residue burning activities, which are totally dependent on the harvesting cycles, crop types, and importantly, land clearing (through the burning of the crop remains). Though observational data is available, it is sparse and spatially constrained, hence satellite data is often used to study over long periods of time and space. In particular, satellite data has proved pivotal in studying, detecting, and analyzing biomass-burning scenarios [28–30].

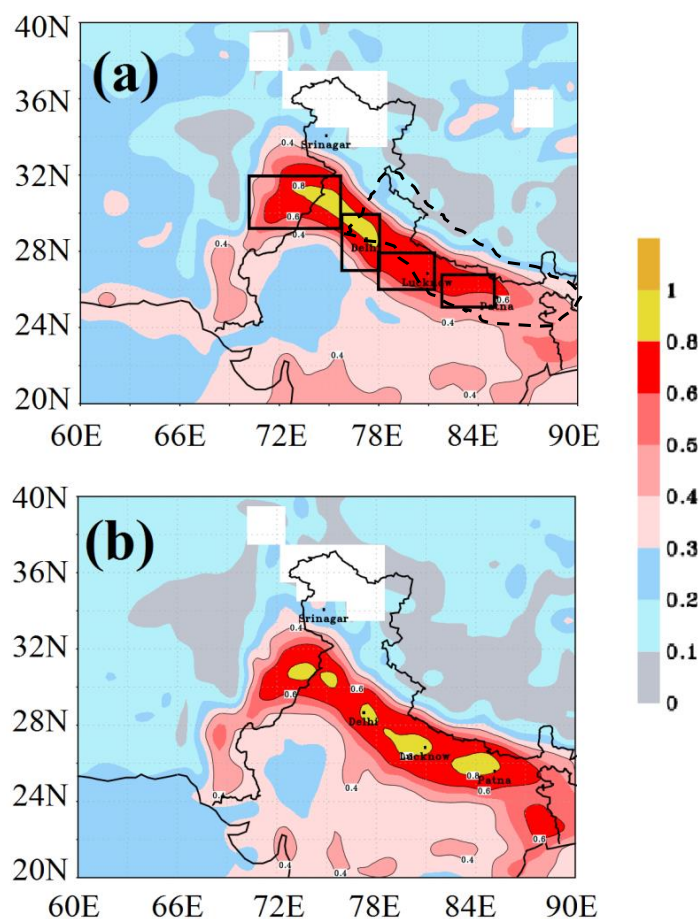


Figure 1. AOD climatology 2002–2019 from MODIS-Aqua (a) October, Boxes here: Northwestern region (70° E–76° E, 29° N–32° N), Delhi region (76° E–78° E, 27° N–31° N), Lucknow region (78° E–81.5° E, 26° N–28° N), and Patna region (82° E–85° E, 25° N–27° N). The dashed line in black marks the boundary of the IGP region. (b) November months over the Indian region (60° E–90° E, 20° N–40° N).

It is also observed from Figure 1 that the entire IGP belt (Punjab region and Delhi region) shows values of AOD of about 0.6. When we analyze Figure 1b for November, the climatological mean AOD values are marked by yellow patches, with AODs as high as 1. High AOD patches are scattered over IGP-created hotspots in the Punjab, Delhi, and Lucknow–Patna regions. Eventually, higher values of AOD are shifted southeastwards. In order to establish and analyze if there was an increasing trend in the AODs and, if so, were there any drastic changes?, we plotted the time series (during the last 15 years) of AOD, as shown in Figure 2a–c, over three different regions: the Northern Indian region (60° E– 90° E, 20° N– 40° N), the Punjab region (74° E– 77° E, 29° N– 32° N), and the Lucknow–Patna region (80° E– 86° E, 25° N– 27° N), respectively.

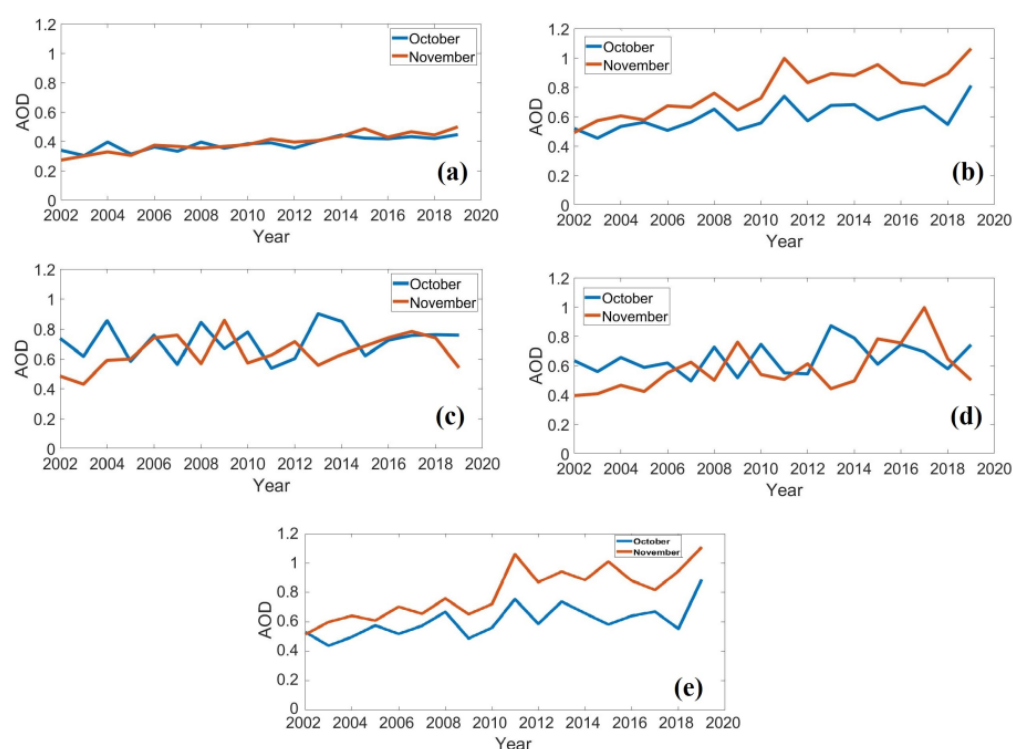


Figure 2. Time series of AOD over (a) Indian region 60° E– 90° E, 20° N– 40° N), (b) Northwestern region (70° E– 76° E, 29° N– 32° N), (c) Delhi region (76° E– 78° E, 27° N– 31° N), (d) Lucknow region (78° E– 81.5° E, 26° N– 28° N), and (e) Patna region (82° E– 85° E, 25° N– 27° N).

Figure 2 reveals quite interesting results. Over the Northern Indian region, the AOD from 2002–2019 during November showed that there was an 83% increase in AOD loading, while during October, the increase was $\sim 30\%$. Figure 2b shows that over the Punjab region, a year-to-year cyclic behavior is observed. In some years, AOD is high (2004, 2008, 2010, 2011, 2013, etc.), while in consecutive years it is low. This may be related to the changing crop pattern or available land area for residual burning [31]. We also observe an increase in November AOD by $\sim 26\%$, but the AODs during October do not show a significant increasing trend. There is an intriguing result as an opposite trend in AOD loading is observed during October and November. The year which shows an increase in AOD during October shows a decrease in AOD during November over the Delhi and Lucknow regions. Figure 2c shows some startling results, over the Lucknow and Patna regions, the increasing trend in AOD during October was $\sim 56\%$, and during November, the increase was by a whopping $\sim 116\%$. In other words, during November, the AOD loading has almost doubled in the last 15 years in this region. AODs shoot up predominantly during biomass burning scenarios and especially during the post-monsoon season. To further investigate the phenomenal rise in the AODs during these time scales, we plotted the spatial variability of fire counts over these regions (Figure 3a–j). Figure 3 shows the spatial distribution of

fire confidence (during October and November) for different confidence ranges (60 to 90) of fires over the Northern Indian region. We clearly observe that during the month of October, the fire counts are centered mostly around the Punjab region, specifically the fire counts with higher confidence >90 and ≤ 100 are centered over the well-known burning regions over Punjab. For the month of November, the fires seem to be widespread over the northern IGP belt.

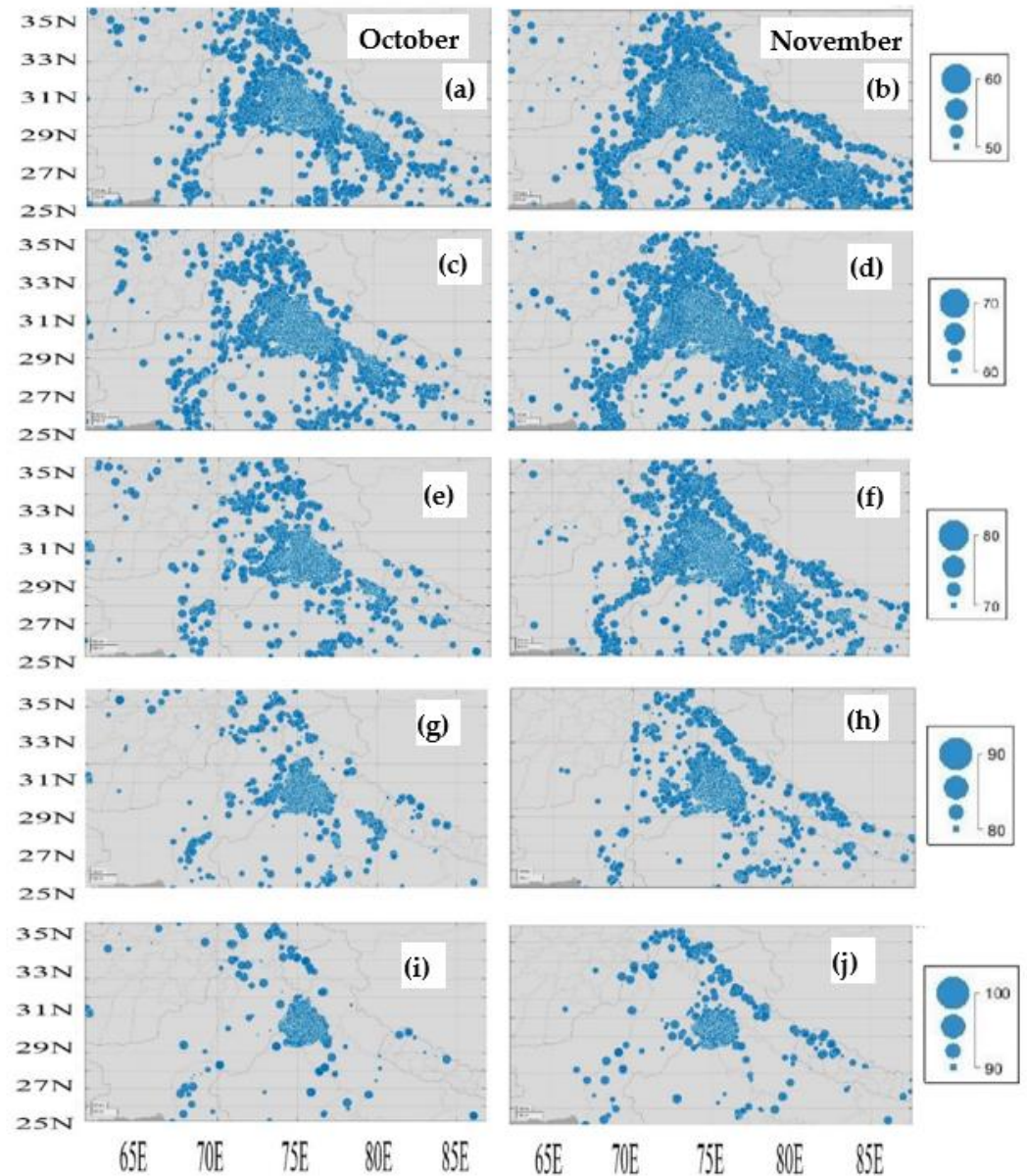


Figure 3. Spatial distribution of Fire confidence from 2002 to 2019 for October and November (a,b) ≥ 50 and ≤ 60 , (c,d) ≥ 60 and ≤ 70 , (e,f) ≥ 70 and ≤ 80 , (g,h) ≥ 80 and ≤ 90 , (i,j) ≥ 90 and ≤ 100 .

The yellow patches with high AODs (Figure 1a,b) corroborate with the patches with higher fire counts (Figure 3a–j). We also observe that the maximum fires belong to the lower confidence range below 70. In November, for all the confidence, there is a NW to SE stretch parallel to IGP and another stretch is along the Indus River in Pakistan from Lahore to Karachi. These stretches of fire are along the rivers. Figure 4a,b, up to j show the number of fire counts during October and November for the Northern Indian Region, the Punjab region, and the Lucknow and Patna regions), respectively.

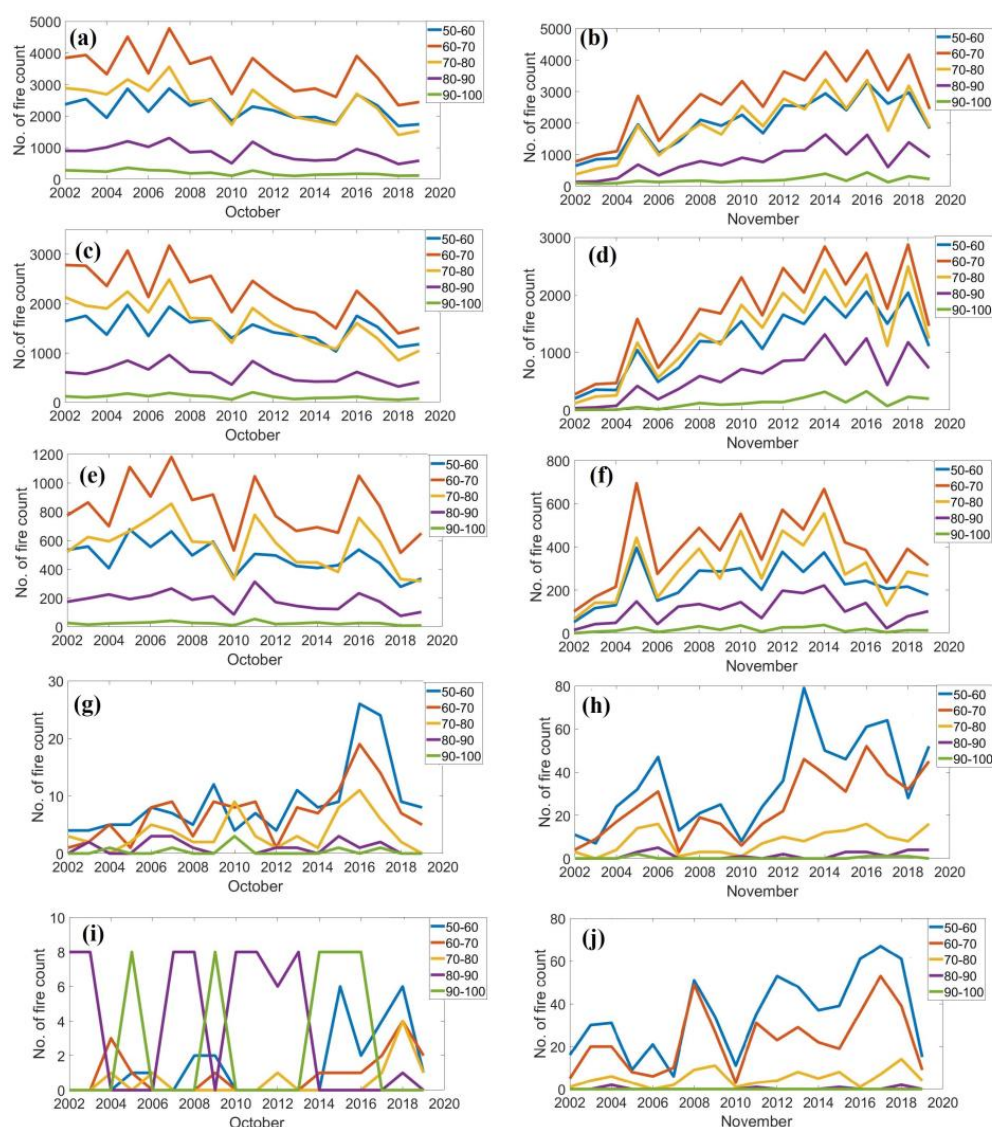


Figure 4. Time series of the number of fire counts in the different fire confidence range in the month of October (a) and November (b) over the Indian region (20–40° N and 60–90° E). Similarly, (c,d) North-western region (70° E–76° E, 29° N–32° N), (e,f) Delhi region (76° E–78° E, 27° N–31° N), (g,h) Lucknow (78° E–81.5° E, 26° N–28N) and (i,j) Patna region (82° E–85° E, 25° N–27° N) respectively.

Table 1 shows the average number of fires for the range of the significance levels based on Figure 3. The confidence level shows tremendous differences over the selected regions of the IGP. The northwestern region of India, which is the region of the origin of the fire and its pollution, shows a great number of fires as compared to other regions in November and October. November is the month when the fire started to bud over the Lucknow and Patna regions, the eastern part of the IGP. Further, wind anomalies in these months played a chief role in spreading the ashes and smoke from the fire over the IGP region.

The annual variation of the fire count is shown in Figure 4. Over the Northern Indian region, a decreasing trend in fire counts is depicted in all confidence levels during the month of October (Figure 4a). While in November, we observe an increasing trend in fire count confidence levels up to 90 and a slightly increasing trend above the confidence level of 90. Hence, the fire count confidence levels indicate that the increase in overall AOD over the Northern Indian region is attributed to the increase in fire counts. Figure 4b illustrates the fire counts over Punjab. During October, we see a decreasing fire count trend (as when compared with the fire counts in the Northern Indian region), while for November, the

fire count shows an increasing trend. Analyzing Figure 4a,b, it can be deduced that the Punjab region seems to control the increase in fire events over the Northern Indian region. Figure 4c displays the fire counts over the Lucknow and Patna regions; during November, the confidence level from 50 to 80 shows an increase, while during October, the trend is a mix of an increase and a decrease in the confidence levels. The results clearly show that the increase in AOD over the Lucknow and Patna regions is related to increasing fire events, though the corroboration is much stronger over the other two regions (Northern India and Punjab). In the scattering and spread of pollution, dust, and smoke, the direction and speed of the regional wind with season play a vital role. It will be interesting to investigate the variability of wind over the IGP region and its surroundings.

Table 1. Total number of fire counts averaged over selected regions of IGP for significant ranges for October and November.

October	50–60	60–70	70–80	80–90	90–100
Indian region	40,033	61,202	43,155	15,152	3537
Northwestern region	26,866	39,944	29,115	10,419	1998
Delhi region	8676	14,743	10,156	3225	438
Lucknow region	160	127	64	20	7
Patna region	25	17	9	63	40
November	50–60	60–70	70–80	80–90	90–100
Indian region	35,962	49,281	35,372	14,742	3527
Northwestern region	21,588	30,448	24,146	1074	2240
Delhi region	4216	7071	5330	1923	310
Lucknow region	628	451	145	26	5
Patna region	625	409	91	6	0

In order to understand the increase in the fire counts over the three principal regions, we also looked into the possible role of the spread of forest fires through the means of wind transportation or long transport due to winds. To do so, we plotted the wind anomalies for the entire period of study (2002–2019), but separated them in order to decipher and delineate them in a more detailed way. On the basis of recent research [32], we split the analysis of the wind anomalies into two different time periods 2002–2009 and 2011–2018, during October, as shown in Figure 5, and during November, as shown in Figure 6. From Figure 5, it is observed that during October, the increase in AOD at the lower IGP belt is due to transport from the northwestern regions (Punjab and Haryana region). One of the significant results we observed from Figure 5 is that during recent years, from 2010 onwards, the winds have become stronger, which indicates that more AOD is getting transported to the lower IGP belt as compared to previous years until 2009. On analyzing Figure 6, we observe that during November, we do not see the transport coming towards the lower IGP region, but in fact, we see a slight turning of these winds towards the central Indian region, which may be taking the AOD into the northwestern region, towards the central Indian region. Hence, during November, it can be deciphered that because of the low wind speeds over the lower IGP belt and the increase in fires, the AODs in the polluted air tend to hover for a longer time than usual.

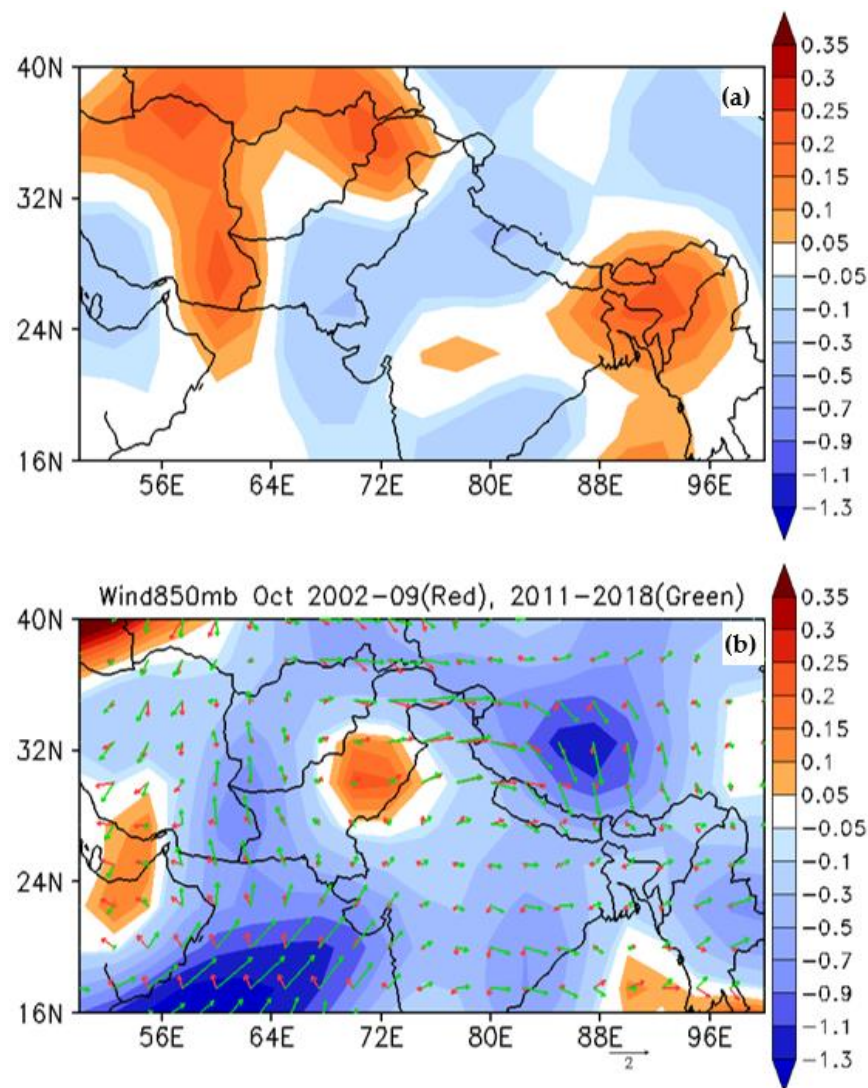


Figure 5. October (a) Vertical velocity (Omega at 900 mb) (b) Winds for two periods and difference in the magnitude of 2002–2009 (wind in red) to 2011–2018 (wind in green).

Though earlier studies have pointed out that an increase in the fire counts is related to the greater availability of crop residue to burn and proportional to the waste generated, which is also proportional to the crop production amounts [22]. In this study, we investigated the causes of the spread of deteriorating unhealthy air over the IGP region. Further, in this first-ever study, we probe and prove the role of wind patterns in the spreading of toxic air throughout the IGP region. Many previous studies pointed out various theories to support that the global wind pattern has been stilling over the past few decades, and many of these studies focused on the drag force of wind speed linked to increased terrestrial roughness caused by urbanization and/or vegetation changes [5,15]. This study found that after 2010, an increasing rate of global wind speeds, i.e., three times the decreasing rate before 2010, countered the previous theories of global wind speed stilling [32]. An interesting fact is that, though terrestrial roughness did not suddenly change in or after 2010, global wind speeds have been showing an increase [33]. Hence, it becomes predominate that the variation in wind speed is determined mainly by driving forces associated with decadal variability of large-scale ocean-atmospheric circulations and not only dependent on terrestrial roughness alone, as was previously thought to be the case.

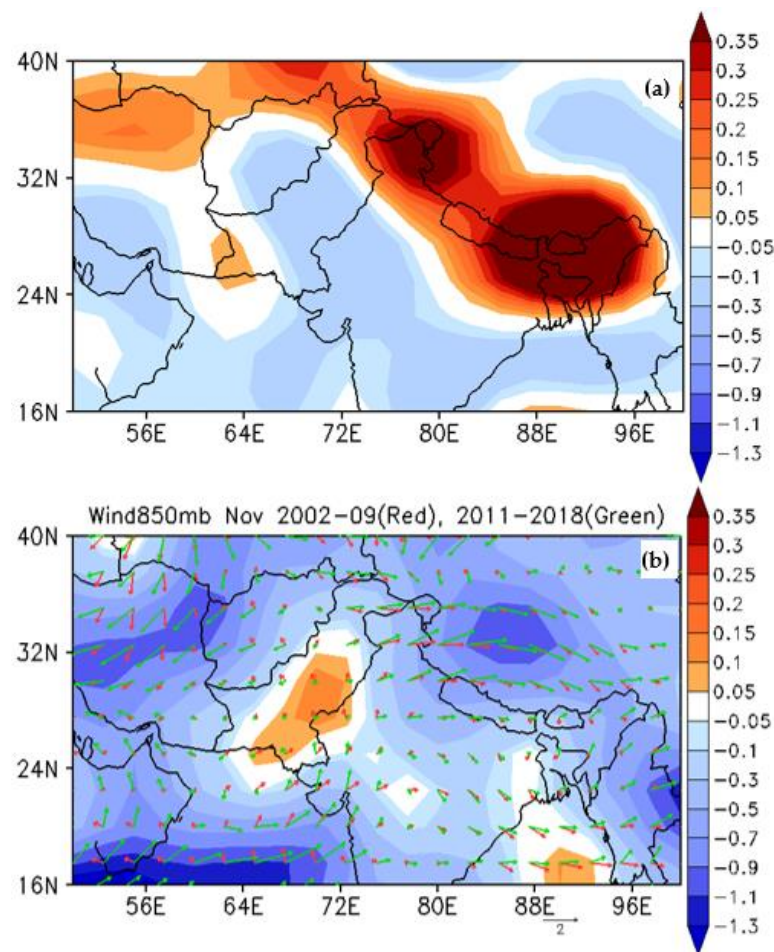


Figure 6. November (a) Vertical velocity (Omega at 900 mb) (b) Winds for two periods and difference in the magnitude of 2002–2009 to 2011–2018.

4. Discussions

An increase in dryness in the lower troposphere causes a decrease in rainfall, dry skin, eye irritation, and health-related ailments (asthma and other respiratory problems). The rainfall and moisture anomalies over the IGP and Indian regions have increased in recent decades (Figure 7a,b), especially during the post-monsoon season. Our study, for the first time, establishes the fact of an increase in wind speed over the IGP region since around 2011 during October–November. Our study also reports the consequences of such increased wind speeds on the spread of harmful pollutants to a wider geographical area. In other words, we propose that increased wind speeds essentially acted as fuel in enhancing the wider spread of harmful pollutants to a wider area than they were during the past few decades. WMO reports indicate a risk of dry conditions over various parts of the Earth due to elevated pollution, increased surface temperature, and decreased humidity. In such conditions of incongruity, we point out that apart from the ground-based infusion of aerosols due to anthropogenic activities, the factors of the atmosphere, i.e., the enhanced wind speeds, become important to be considered while reaching the decision that determines the fate of regional climate variability in a region like IGP.

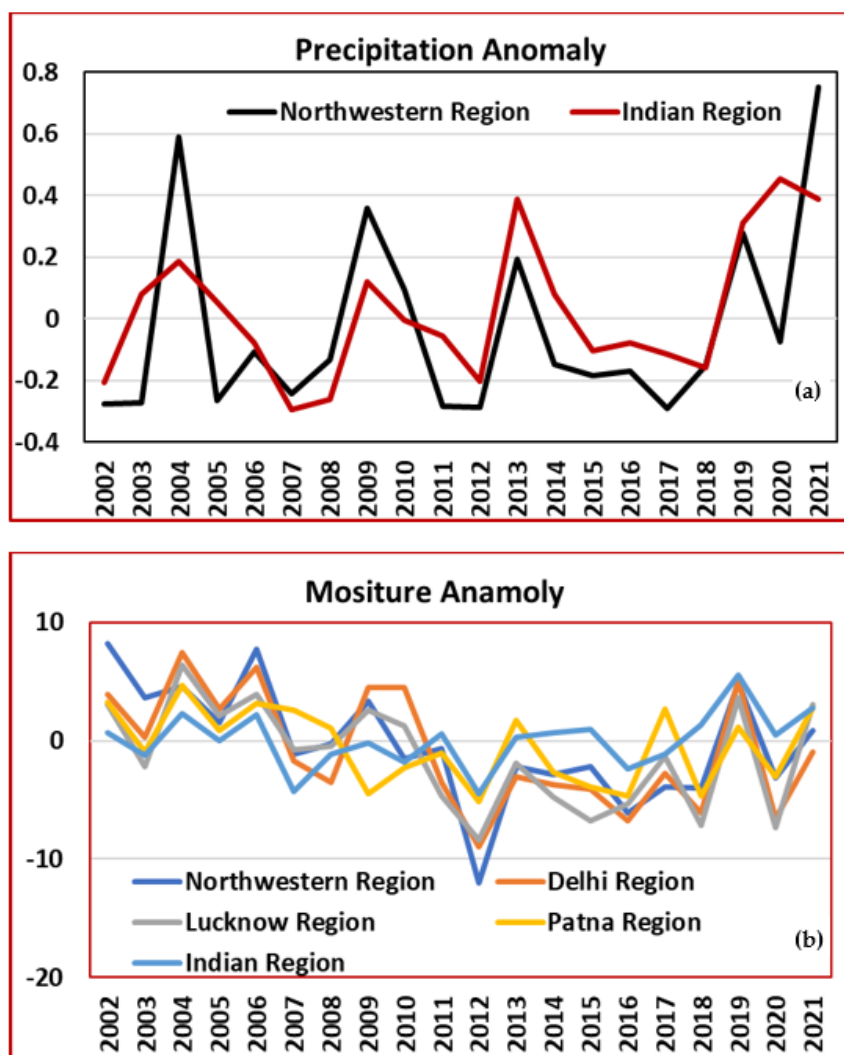


Figure 7. Averaged variables over selected regions of IGP for October and November from 2002 to 2021 (a) Rainfall anomaly (mm/day) (b) Moisture anomaly (%).

5. Conclusions

The spread of aerosol from fires was studied using monthly data from MODIS over the Indo-Gangetic Plain (IGP). Every year, rice is harvested during October and November. In addition, to keep spirits high for crop production, the community has many festival celebrations during this time. Along with the festival's celebration, forest fires and stubble burning have become common practices among farmers and local communities. The fire counts have increased drastically in all confidence ranges (50–100%) in November and a widespread increase in the fires with a confidence level above 60 to 80 % over the whole Northern Indian region is observed. AOD also shows an increase with values > 0.7 over the northwestern and IGP regions. There have been some startling results over the lower IGP belt, where there has been an increasing trend in AOD during October, to the alarming rate of ~56%, and during November, the increase was by a whopping ~116 %. Transporting factors from winds have become stronger, which indicates more AOD has been transported to the lower IGP belt since 2009 October. However, in November, we did not find the transport coming towards the lower IGP region, but, in fact, we saw a slight turning of these winds towards the central Indian region, which may be taking the AOD in the northwestern region towards the central Indian region. Hence, during November, it is inferred that due to the low wind speed over the lower IGP belt and the increase in fires (i.e., AODs), the polluted air tends to linger for a long time.

Author Contributions: Conceptualization, R.L.B. and V.K.; methodology, R.L.B.; software, R.P., R.L.B. and V.K.; validation, P.R.C.R.; formal analysis and editing, R.L.B., P.R.C.R. and V.K.; investigation, V.K.; resources, V.K. and R.P.; data curation, R.P.; writing—original draft preparation, P.R.C.R.; writing—review and editing, P.R.C.R., R.L.B. and V.K.; visualization, R.P., V.K. and R.L.B.; supervision, S.Y.; project administration, R.L.B.; funding acquisition, V.K. and S.Y. All authors have read and agreed to the published version of the manuscript.

Funding: This research received no external funding.

Institutional Review Board Statement: Not applicable.

Informed Consent Statement: Not applicable.

Data Availability Statement: In All the datasets are acquired from public resources and available online.

Acknowledgments: The authors are grateful to the MODIS, ERA-Interim, and CALIPSO product developers. The authors are also thankful to the online websites for providing various datasets and making them available to use in the present study.

Conflicts of Interest: The authors declare no conflict of interest.

References

1. Saikawa, E.; Panday, A.; Kang, S.; Gautam, R.; Zusman, E.; Cong, Z.; Somanathan, E.; Adhikary, B. Air Pollution in the Hindu Kush Himalaya. In *The Hindu Kush Himalaya Assessment: Mountains, Climate Change, Sustainability and People*; Wester, P., Mishra, A., Mukherji, A., Shrestha, A.B., Eds.; Springer International Publishing: Cham, Switzerland, 2019; pp. 339–387. [\[CrossRef\]](#)
2. Lee, W.-S.; Bhawar, R.L.; Kim, M.-K.; Sang, J. Study of aerosol effect on accelerated snow melting over the Tibetan Plateau during boreal spring, 2013. *Atmos. Environ.* **2013**, *75*, 113–122. [\[CrossRef\]](#)
3. Rahul, P.R.C.; Bhawar, R.L.; Ayantika, D.C.; Panicker, A.S.; Safai, P.D.; Tharaprabhakaran, V.; Padmakumari, B.; Raju, M.P. Double blanket effect caused by two layers of black carbon aerosols escalates warming in the Brahmaputra River Valley. *Sci. Rep.* **2014**, *4*, 3670. [\[CrossRef\]](#) [\[PubMed\]](#)
4. Taylor, D. Biomass burning, humans and climate change in Southeast Asia. *Biodivers. Conserv.* **2010**, *19*, 1025–1042. [\[CrossRef\]](#)
5. Jethva, H.; Chand, D.; Torres, O.; Gupta, P.; Lyapustin, A.; Patadia, F. Agricultural Burning and Air Quality over Northern India: A Synergistic Analysis using NASA's A-train Satellite Data and Ground Measurements. *Aerosol Air Qual. Res.* **2018**, *18*, 1756–1773. [\[CrossRef\]](#)
6. Vaishya, A.; Singh, P.; Rastogi, S.; Babu, S.S. Aerosol black carbon quantification in the central Indo-Gangetic Plain: Seasonal heterogeneity and source apportionment. *Atmos. Res.* **2017**, *185*, 13–21. [\[CrossRef\]](#)
7. Vadrevu, K.P.; Csiszar, I.; Ellicott, E.; Giglio, L.; Badarinath, K.V.S.; Vermote, E.; Justice, C. Hotspot analysis of vegetation fires and intensity in the Indian region. *IEEE J. Sel. Top. Appl. Earth Obs. Remote Sens.* **2013**, *6*, 224–238. [\[CrossRef\]](#)
8. Kaskaoutis, D.G.; Kumar, S.; Sharma, D.; Singh, R.P.; Kharol, S.K.; Sharma, M.; Singh, A.K.; Singh, S.; Singh, A.; Singh, D. Effects of crop residue burning on aerosol properties, plume characteristics, and long-range transport over northern India. *J. Geophys. Res.* **2014**, *119*, 5424–5444. [\[CrossRef\]](#)
9. Vermote, E.; Ellicott, E.; Dubovik, O.; Lapyonok, T.; Chin, M.; Giglio, L.; Roberts, G.J. An approach to estimate global biomass burning emissions of organic and black carbon from MODIS fire radiative power. *J. Geophys. Res.* **2009**, *114*, D18205. [\[CrossRef\]](#)
10. Jacobson, M.Z. Effects of biomass burning on climate, accounting for heat and moisture fluxes, black and brown carbon, and cloud absorption effects. *J. Geophys. Res. Atmos.* **2014**, *119*, 8980–9002. [\[CrossRef\]](#)
11. Garrett, T.J.; Avey, L.; Palmer, P.I.; Stohl, A.; Neuman, J.A.; Brock, C.A.; Holloway, J.S. Quantifying wet scavenging processes in aircraft observations of nitric acid and cloud condensation nuclei. *J. Geophys. Res.* **2006**, *111*, D23S51. [\[CrossRef\]](#)
12. Ramanathan, V.; Carmichael, G.R. Global and regional climate changes due to black carbon. *Nature* **2008**, *1*, 221–227.
13. Fujii, Y.; Kawamoto, H.; Tohno, S.; Oda, M.; Iriana, W.; Lestari, P. Characteristics of carbonaceous aerosols emitted from peatland fire in Riau, Sumatra, Indonesia (2): Identification of organic compounds. *Atmos. Environ.* **2015**, *110*, 1–7. [\[CrossRef\]](#)
14. Zhao, C.; Garrett, T.J. Effects of Arctic haze on surface cloud radiative forcing. *Geophys. Res. Lett.* **2015**, *42*, 557–564. [\[CrossRef\]](#)
15. Grandey, B.S.; Lee, H.-H.; Wang, C. Radiative effects of interannually varying vs. interannually invariant aerosol emissions from fires. *Atmospheric Chem. Phys.* **2016**, *16*, 14495–14513. [\[CrossRef\]](#)
16. Zhao, H.; Che, H.; Xia, X.; Wang, Y.; Wang, H.; Wang, P.; Ma, Y.; Yang, H.; Liu, Y.; Wang, Y.; et al. Multiyear Ground-Based Measurements of Aerosol Optical Properties and Direct Radiative Effect over Different Surface Types in Northeastern China. *J. Geophys. Res. Atmos.* **2018**, *123*, 13887–13916. [\[CrossRef\]](#)
17. Crippa, P.; Castruccio, S.; Archer-Nicholls, S.; Lebron, G.B.; Kuwata, M.; Thota, A.; Sumin, S.; Butt, E.; Wiedinmyer, C.; Spracklen, D.V. Population exposure to hazardous air quality due to the 2015 fires in Equatorial Asia. *Sci. Rep.* **2016**, *6*, 37074. [\[CrossRef\]](#) [\[PubMed\]](#)
18. Badarinath, K.V.S.; Kumar Kharol, S.; Rani Sharma, A. Long-range transport of aerosols from agriculture crop residue burning in Indo-Gangetic Plains—A study using LIDAR, ground measurements and satellite data. *J. Atmos. Sol. Terr. Phys.* **2009**, *71*, 112–120. [\[CrossRef\]](#)

19. Bhawar, R.L.; Fadnavis, S.; Kumar, V.; Rahul, P.R.C.; Sinha, T.; Lolli, S. Radiative Impacts of Aerosols During COVID-19 Lockdown Period Over the Indian Region. *Front. Environ. Sci.* **2021**, *9*, 746090. [[CrossRef](#)]
20. Ito, A.; Penner, J.E. Global estimates of biomass burning emissions based on satellite imagery for the year 2000. *J. Geophys. Res.* **2004**, *109*, D14S05. [[CrossRef](#)]
21. Mitchell, R.M.; O'Brien, D.M.; Campbell, S.K. Characteristics and radiative impact of the aerosol generated by the Canberra firestorm of January 2003. *J. Geophys. Res.* **2006**, *111*, D02204. [[CrossRef](#)]
22. Jethva, H.; Torres, O.; Field, R.D.; Lyapustin, A.; Gautam, R.; Kayetha, V. Connecting Crop Productivity, Residue Fires, and Air Quality over Northern India. *Sci. Rep.* **2019**, *9*, 16594. [[CrossRef](#)] [[PubMed](#)]
23. Vijayakumar, K.; Safai, P.D.; Devara, P.C.S.; Rao, S.V.B.; Jayasankar, C.K. Effects of agriculture crop residue burning on aerosol properties and long-range transport over northern India: A study using satellite data and model simulations. *Atmos. Res.* **2016**, *178–179*, 155–163. [[CrossRef](#)]
24. Jethva, H.; Torres, O. Satellite-based evidence of wavelength-dependent aerosol absorption in biomass burning smoke inferred from Ozone Monitoring Instrument. *Atmospheric Chem. Phys.* **2011**, *11*, 10541–10551. [[CrossRef](#)]
25. Kaufman, Y.J.; Tanre, D.; Remer, L.; Vermote, E.; Chu, A.; Holben, B.N. Operational remote sensing of tropospheric aerosol over land from EOS moderate resolution imaging spectroradiometer. *J. Geophys. Res. Atmos.* **1997**, *102*, 17051–17067. [[CrossRef](#)]
26. Remer, L.A.; Kaufman, Y.J.; Tanré, D.; Mattoo, S.; Chu, D.A.; Martins, J.V.; Li, R.-R.; Ichoku, C.; Levy, R.C.; Kleidman, R.G.; et al. The MODIS aerosol algorithm, products, and validation. *J. Atmos. Sci.* **2005**, *62*, 947–973. [[CrossRef](#)]
27. Shaik, D.S.; Kant, Y.; Mitra, D.; Singh, A.; Chandola, H.C.; Sateesh, M.; Babu, S.S.; Chauhan, P. Impact of biomass burning on regional aerosol optical properties: A case study over northern India. *J. Environ. Manag.* **2019**, *244*, 328–343. [[CrossRef](#)] [[PubMed](#)]
28. Torres, O.; Chen, Z.; Jethva, H.; Ahn, C.; Freitas, S.R.; Bhartia, P.K. OMI and MODIS observations of the anomalous 2008–2009 Southern Hemisphere biomass burning seasons. *Atmos. Chem. Phys. Discuss.* **2010**, *10*, 3505–3513. [[CrossRef](#)]
29. Sahu, L.K.; Sheel, V.; Pandey, K.; Yadav, R.; Saxena, P.; Gunthe, S. Regional biomass burning trends in India: Analysis of satellite fire data. *J. Earth Syst. Sci.* **2015**, *124*, 1377–1387. [[CrossRef](#)]
30. Roberts, G.; Wooster, M.J.; Lagoudakis, E. Annual and diurnal african biomass burning temporal dynamics. *Biogeosciences* **2009**, *6*, 849–866. [[CrossRef](#)]
31. Shyamsundar, P.; Springer, N.P.; Tallis, H.; Polasky, S.; Jat, M.L.; Sidhu, H.S.; Krishnapriya, P.P.; Skiba, N.; Ginn, W.; Ahuja, V.; et al. Fields on fire: Alternatives to crop residue burning in India. *Science* **2019**, *6453*, 536–538. [[CrossRef](#)] [[PubMed](#)]
32. Vautard, R.; Cattiaux, J.; You, P.; Thépaut, J.N.; Ciais, P. Northern Hemisphere atmospheric stilling partly attributed to an increase in surface roughness. *Nat. Geosci.* **2010**, *3*, 756–761. [[CrossRef](#)]
33. Zeng, Z.; Ziegler, A.D.; Searchinger, T.; Yang, L.; Chen, A.; Ju, K.; Piao, S.; Li, L.Z.X.; Ciais, P.; Chen, D.; et al. A reversal in global terrestrial stilling and its implications for wind energy production. *Nat. Clim. Chang.* **2019**, *9*, 979–985. [[CrossRef](#)]